



ELSEVIER

Thermochimica Acta 280/281 (1996) 191–204

thermochimica
acta

Surface nucleation of μ -cordierite in cordierite glass: thermodynamic aspects¹

R. Müller^{a,*}, R. Naumann^b, S. Reinsch^a

^a Federal Institute of Materials Research and Testing (BAM) Rudower Chaussee 5 (Haus 8.15),
D-12489 Berlin, Germany

^b SETARAM SA, Mendelejewstr. 5, D-09599 Freiberg, Germany

Abstract

The heterogeneous nucleation rate of μ -cordierite at the surface of cordierite glass ($2\text{MgO}\cdot 2\text{Al}_2\text{O}_3\cdot 5\text{SiO}_2$) is discussed in terms of classical nucleation theory (CNT). Calculations are based on experimental viscosity data and estimates of the melting temperature and melting enthalpy of μ -cordierite from calorimetric measurements.

A virtual melting temperature of the metastable μ -cordierite, T_M^μ , was estimated, by means of X-ray measurements, from the primary occurrence of μ -cordierite after brief thermal treatment. T_M^μ was found to lie in the range 1300–1467°C. The molar enthalpy of melting, ΔH_M^μ , was calculated from calorimetric measurements and literature data. Referring to the molar weight of the formula unit, $M = 585 \text{ g mol}^{-1}$, ΔH_M^μ could be narrowed to the range 170–190 kJ mol⁻¹.

The heterogeneous volume nucleation rate, $I^*(T)$, was estimated from the apparent nucleation rate of μ -cordierite which was previously studied at fractured and polished surfaces of cordierite glass by means of transmitting light microscopy. $I^*(T)$ steadily increases up to 235 K above the glass transition temperature at 815°C without reaching a maximum. In the present paper, this exceptional temperature-dependence is discussed in terms of CNT. The best fit of experimental data was obtained for $T_M^\mu \approx 1467^\circ\text{C}$, a low liquid-crystal interfacial free energy, σ , and a low activity of nucleating substrates, Φ , if $\sigma\Phi^{1/3} \approx 100 \text{ mJ m}^{-2}$ is valid.

Keywords: Classical nucleation theory; μ -Cordierite; Cordierite glass; High-temperature calorimetry; Melting temperature; Melting enthalpy; $2\text{MgO}\cdot 2\text{Al}_2\text{O}_3\cdot 5\text{SiO}_2$; Surface nucleation; Viscosity

* Corresponding author.

¹ Dedicated to Professor Hiroshi Suga.

1. Introduction

Metastable high-quartz solid solution (“ μ -cordierite”) crystals frequently occur as the primary crystalline phase when glasses of the ternary system $\text{MgO} \cdot \text{Al}_2\text{O}_3 \cdot \text{SiO}_2$ are allowed to crystallize [1]. Although the crystallization of μ -cordierite is usually followed by the crystallization of the hexagonal high temperature polymorph of cordierite (“ α -cordierite”), which slowly transforms to orthorhombic cordierite below 1450°C [2], the primary μ -cordierite decisively influences overall crystallization of glasses which are of interest for the manufacture of cordierite-based glass or sinter-glass ceramics.

Against that background, the surface-induced nucleation of μ -cordierite has been investigated for glasses of the cordierite stoichiometry ($2\text{MgO} \cdot 2\text{Al}_2\text{O}_3 \cdot 5\text{SiO}_2$) [3–6]. A constant surface nucleation density of μ -cordierite, N^μ , was found not to be influenced by thermal nucleation treatments but by prior surface preparation. A similar effect was reported for float glass surfaces [7]. This behaviour arises from the fact that nucleation of μ -cordierite occurs from a limited number of active surface nucleation sites. All these sites have been exhausted before any crystal can reach detectable size. Thus, N^μ simply represents the number density of active nucleation sites, N_0^μ . Despite this strong saturation effect, it was possible to obtain the surface nucleation rate, dN^μ/dt , utilizing the observed distribution of crystal radii [8–10]. It was remarkable to find dN^μ/dt steadily increasing up to 1050°C (235 K above the glass transition temperature at 815°C) without reaching a maximum.

In the present paper, this effect is discussed in terms of classical nucleation theory (CNT) based on viscosity data and the estimation of the melting temperature and melting enthalpy of μ -cordierite from calorimetric measurements and literature data.

2. Experimental

2.1. Preparation

Batches of the nominal composition of cordierite (wt%: 13.8 MgO, 34.9 Al_2O_3 , 51.3 SiO_2) were melted for 8 h at 1590°C in a Pt crucible. Plates of $\approx 10 \times 15 \times 1 \text{ cm}^3$ and frits were prepared from the melt by casting onto steel plates and pouring into distilled water, respectively. Chemical analysis of the quenched glasses showed that no oxide component deviates more than 0.8 wt% from the nominal composition. Glass powders were prepared by crushing in a metal mortar and subsequent milling and sieving.

Brief isothermal treatments were carried out in a specially designed vertical tube furnace. The device enables movement of the specimen holder within a linear thermal gradient (300°C – 1500°C over a length of 600 mm). Due to the small heat capacity of samples ($< 500 \text{ mg}$) and specimen holder, short heating times were attained enabling “isothermal” brief thermal treatment for periods down to 0.5 min.

Samples of μ - and α -cordierite were crystallized from glass powders 6–11 μm in size by heating of 10 K min^{-1} to 1000°C and 1200°C , respectively. The final temperatures were inferred from corresponding DTA curves, which show quite distinct exothermic peaks for the crystallization of μ - and α -cordierite [11]. The completeness of overall

crystallization was confirmed by subsequent DTA runs of these samples. One or no exothermic peak was found for the μ -cordierite or α -cordierite samples, respectively.

2.2. Measurements

Glass cuboids $5 \times 5 \times 1 \text{ mm}^3$ in size were used for viscosity measurements under three-point bending symmetry between 780°C and 920°C . Above 920°C the crystallization of μ -cordierite prevents any further measurements. Additional viscosity measurements were carried out between 1500°C and 1600°C using a Haake high-temperature rotational viscometer. The density of bulk glass samples was measured by means of Archimedes' method at 25°C . A Leitz vitreous silica dilatometer of the tube type (horizontal arrangement) was used for measuring the coefficient of thermal expansion. Enthalpy differences between glass, μ - and α -cordierite were measured by means of a Setaram HT 1500 high-temperature calorimeter. Samples were dropped from room temperature (25°C) into the measuring cell that was held at measuring temperature within an accuracy of $\pm 1 \text{ K}$ [12]. Enthalpy calibration was made using sapphire as reference material. All measurements were repeated at least five times.

3. Results

3.1. Physical properties

The influence of the temperature on the viscosity of the glasses used in the present study, $\eta(T)$, can be well fitted in terms of the Vogel–Fulcher–Tamman equation, $\lg \eta(T) = A + B/(T - C)$, with $A = -1.96$, $B = 4265 \text{ K}$, and $C = 777 \text{ K}$.

A density of $2.60 \pm 0.01 \text{ g cm}^{-3}$ was found for the cordierite glass samples. The result confirms previously published literature data for glasses of exact cordierite stoichiometry (2.7 g cm^{-3} [13], 2.71 g cm^{-3} [14], 2.46 g cm^{-3} [15], 2.59 g cm^{-3} [16]). The density of μ -cordierite (2.58 g cm^{-3} [14], 2.6 g cm^{-3} [17]) is very close to that of parent glass. A more pronounced deviation is evident for the density of α -cordierite (2.495 g cm^{-3} [15]). One should note that, in the present case, the density is decreasing in the course of crystallization.

The coefficient of thermal expansion (CTE) of cordierite glass was found to be $3.77 \pm 0.01 \times 10^{-6} \text{ K}^{-1}$ (20°C – 400°C). This result well confirms CTE data given in Ref. [13] ($3.8 \times 10^{-6} \text{ K}^{-1}$ for 20°C – 800°C). The glass transition temperature was found to be 815°C . Low CTE values are reported also for μ -cordierite ($2.87 \times 10^{-6} \text{ K}^{-1}$ (20°C – 600°C) [15]; $2.47 \times 10^{-6} \text{ K}^{-1}$ (20°C – 600°C) [18]) and α -cordierite ($0.9 \times 10^{-6} \text{ K}^{-1}$ (20°C – 800°C) [18]). Thus, it seems to be justified to use room temperature density values for the glass ($\approx 2.60 \text{ g cm}^{-3}$) and μ -cordierite ($\approx 2.59 \text{ g cm}^{-3}$) as a good approximation in calculating nucleation rates.

3.2. Melting temperature, T_M^μ

The melting temperature of μ -cordierite, T_M^μ , cannot be measured. No thermal equilibrium can be attained between metastable μ -cordierite crystals and melt because

any thermal treatment progressively reduces the amount of the originally crystallized μ -cordierite while that of α -cordierite simultaneously increases. Alternatively, a virtual T_M^μ can be estimated taking into account that no μ -cordierite can crystallize above this temperature. Therefore no μ -cordierite should be detectable even during the early stage of brief thermal treatments at $T > T_M^\mu$. The detectable amount of μ -cordierite is limited, however, by two effects that could generate a value of T_M^μ that is too low:

- (1) The decomposition rate of μ -cordierite is progressively increasing with increasing temperature. That makes it more difficult to find the maximum amount of temporarily formed μ -cordierite.
- (2) The crystallization of both μ - and α -cordierite starts from the surface causing an inner layer of μ -cordierite and an outer layer of α -cordierite concentrically growing into the bulk [11]. Thus, a μ -cordierite layer of a given thickness yields a lower volume fraction for glass particles than for small ones.

Therefore, glass powders of 160–200 μm in size were quickly heated, held for a time, t_w , at the temperature, T_w , quenched in air and studied by X-ray powder diffraction. t_w was tuned to T_w to ensure a thickness of the crystalline surface layer of $\approx 100 \mu\text{m}$ that is comparable to the mean radius of glass powder particles. In this way primary crystallization of μ -cordierite was detectable up to 1300°C. In any case X-ray diffraction patterns were found in Ref. [19] to be very close to those reported in Ref. [1] for μ -cordierite of the stoichiometric composition.

No experiments were performed at $T > 1300^\circ\text{C}$ due to the progressive occurrence of mullite crystals and the compositional change of the melt which is expected for this situation. Assuming that T_M^μ does not lie beyond the melting temperature of the stable orthorhombic polymorph of cordierite at $1467 \pm 10^\circ\text{C}$ [20], T_M^μ can be anticipated to lie in the range 1300°C–1467°C.

3.3. Melting enthalpy, ΔH_M^μ

Fig. 1 shows the temperature-dependence of enthalpy, $H(T)$, of cordierite glass (curve g), the melt (m), μ -cordierite (μ), α -cordierite (α) and orthorhombic cordierite (C). All enthalpy data are related to the enthalpy of orthorhombic cordierite at 25°C which is set to zero.

3.3.1. Calculation of curves

- (1) The calculation of $H(T)$ curves in Fig. 1 is based on literature data of the specific heat capacity, $C_p(T)$, for cordierite glass, the melt and orthorhombic cordierite [20, 21]. $C_p(T)$ was found to follow Eq. (1) for the c_i values listed in Table 1.

$$C_p(T) = c_0 + c_1 T + c_2 T^{-0.5} + c_3 T^{-2} \quad (1)$$

$H(T)$ curves were calculated by numerical integration of Eq. (1). $C_p(T)$ data of orthorhombic cordierite were used for all crystalline phases. Thus, parallel curves were obtained for H_μ , H_α , and H_C .

- (2) Integration of Eq. (1) cannot yield any enthalpy differences between two phases (i.e. phases i and j at $T = 25^\circ\text{C}$, $H_{i-j}(25^\circ\text{C})$). For that reason, samples of glass (g),

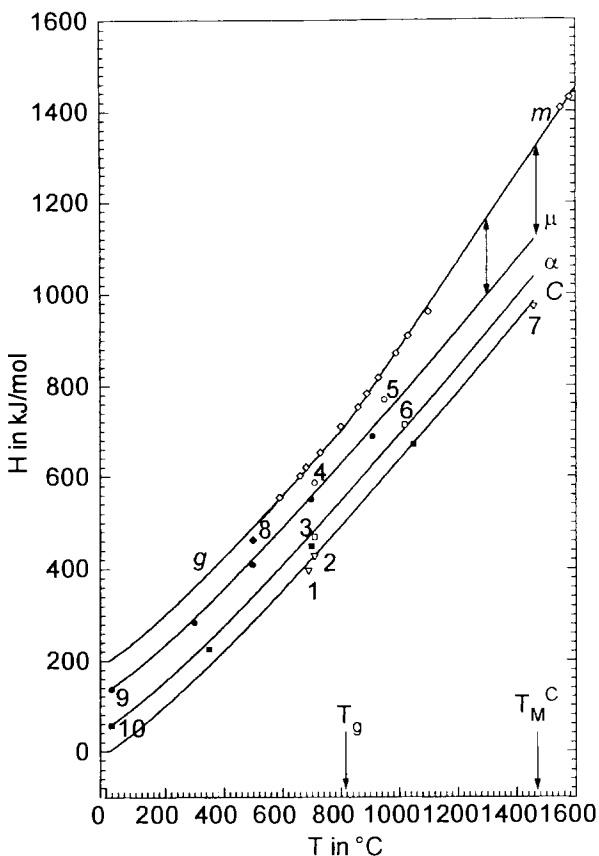


Fig. 1. Enthalpy, H , of cordierite glass (g), melt (m), μ -cordierite (μ), α -cordierite (α) and orthorhombic cordierite (C) at $T = 25^\circ\text{C}$ as a function of temperature. All enthalpy data are related to the enthalpy of orthorhombic cordierite at 25°C which is set to zero. For points see Table 2. Double arrows: melting enthalpy of μ -cordierite. Lower arrows: T_M^C = melting temperature of orthorhombic cordierite at 1467°C [20]; T_g = glass transition temperature at 815°C .

μ -cordierite (μ) and α -cordierite (α) were heated from 25°C to 1200°C by dropping them into the measuring cell of a high-temperature calorimeter. The consumed heat for samples g, μ and α was found to be $\Delta Q_g = 844 \text{ J g}^{-1}$, $\Delta Q_\mu = 955 \text{ J g}^{-1}$ and $\Delta Q_\alpha = 639 \text{ J g}^{-1}$, respectively. $\Delta H_g = 494 \text{ kJ mol}^{-1}$, $\Delta H_\mu = 559 \text{ kJ mol}^{-1}$ and $\Delta H_\alpha = 639 \text{ kJ mol}^{-1}$ results for the molar weight of the formula unit, $M = 585 \text{ g mol}^{-1}$. It was proved by DTA runs of analogously pre-treated samples that all dropping experiments caused almost complete crystallization of α -cordierite. Hence, the same enthalpy value, $H_\alpha(1200^\circ\text{C})$, was reached in all three cases and the consumed heat can be written as follows: $\Delta H_g = H_\alpha(1200^\circ\text{C}) - H_g(25^\circ\text{C})$, $\Delta H_\mu = H_\alpha(1200^\circ\text{C}) - H_\mu(25^\circ\text{C})$ and $\Delta H_\alpha = H_\alpha(1200^\circ\text{C}) - H_\alpha(25^\circ\text{C})$. Finally, one gets $\Delta H_{\mu-\alpha}(25^\circ\text{C}) = 81 \text{ kJ mol}^{-1}$ and $\Delta H_{g-\mu}$

Table 1
Heat capacity data used in Eq. (1)

Phase	c_0	c_1	c_2	c_3	Ref.
Melt	874.406	0.047168	0	0	[20]
Glass	582.082	0.143690	0	-1.4584×10^7	[20]
Orthorhombic	821.340	0.043339	-5000.3	-8.2112×10^6	[21]

(25°C) = 64 kJ mol⁻¹. Taking account of temperature-dependence of the calculated $H_i(T)$ curves, $\Delta H_{\alpha-C}(25^\circ\text{C}) = 55 \text{ kJ mol}^{-1}$ results from the melting enthalpy of orthorhombic cordierite, $\Delta H_M^C = \Delta H_{mC}(1467^\circ\text{C}) = 345 \text{ kJ mol}^{-1}$ reported in [20].

3.3.2. Experimental points

In Fig. 1 further independently obtained experimental values (solid points) and literature data (open points) are summarized. The origin of each point is explained in Table 2. Two types of data are involved: enthalpy differences between phases i and j at a given temperature, $\Delta H_{i-j}(T)$, and enthalpy differences between two temperatures for a given phase, $\Delta H_i(T_1-T_2)$. For the sake of greater clarity, all enthalpy differences are shown as single points in Fig. 1. The points are related to the corresponding value of the nearest neighbour upper $H_j(T)$ curve ($\Delta H_{i-j}(T)$ data points) or to the $H_i(25^\circ\text{C})$ value of the corresponding $H_i(T)$ curve ($\Delta H_i(T_1-T_2)$ data points). As shown in Fig. 1, all experimental data well confirm the calculated $H_i(T)$ curves. The use of identical $C_p(T)$ data for all crystalline phases seems to be a sufficient approximation.

3.3.3. Melting enthalpy of μ -cordierite, ΔH_M^μ

The melting enthalpy of μ -cordierite, ΔH_M^μ , can be inferred from Fig. 1 as the enthalpy difference between μ -cordierite and melt at $T = T_M^\mu$. The possible range of ΔH_M^μ that is linked to the uncertainty of T_M^μ ($T_M^\mu = 1300\text{--}1467^\circ\text{C}$) is illustrated by the double arrows in Fig. 1. The specific heat of melting, ΔQ_M^μ , was found to be $\Delta Q_M^\mu = 290\text{--}324 \text{ J g}^{-1}$ that yields $\Delta H_M^\mu = 170\text{--}190 \text{ kJ mol}^{-1}$ for $M = 585 \text{ g mol}^{-1}$.

4. Discussion

4.1. Basic equations

In terms of classical nucleation theory (CNT), the steady state homogeneous nucleation rate, $I(T)$, can be sufficiently approximated as [22]:

$$I(T) \approx \frac{kT}{3\pi\lambda^3\eta(T)} n_0 \exp\left(-\frac{W(T)}{kT}\right) \quad (2)$$

where λ is the mean jump distance of molecular building units of the crystallizing component; n_0 is their number per unit volume and $\eta(T)$ is the viscosity of the melt. n_0 is

Table 2

Explanation of experimental enthalpy data (points) in Fig. 1. Open points: literature data, solid points: this work; \blacklozenge , \circ : melt; \bullet , \square : μ -cordierite; \blacksquare , \square : α -cordierite; ∇ : orthorhombic cordierite. All data are related to the molar weight of the formula unit ($2\text{MgO}\cdot 2\text{Al}_2\text{O}_3\cdot 5\text{SiO}_2$), $M = 585 \text{ g mol}^{-1}$. ΔH and T are given in kJ mol^{-1} and $^\circ\text{C}$, respectively. $\Delta H_{i,j}(T)$ = difference of enthalpy between phases i and j at the temperature T ; $\Delta H_i(T_1-T_2)$ = difference of enthalpy between temperatures T_1 and T_2 for phase i . Points 7, 9 and 10 were used to determine the ordinates of the calculated $H(T)$ curves

Data point	Property	Method	Ref.
∇ 1	$\Delta H_{g,c}(690) = 226$	Differences of heat of solution in $\text{PbO}\cdot\text{B}_2\text{O}_3$ melts	[23]
∇ 2	$\Delta H_{g,c}(708) = 208.9$	Differences of heat of solution in $\text{PbO}\cdot\text{B}_2\text{O}_3$ melts	[24]
\square 3	$\Delta H_{g,\alpha}(708) = 167.9$	Differences of heat of solution in $\text{PbO}\cdot\text{B}_2\text{O}_3$ melts	[24]
\circ 4	$\Delta H_{g,\mu}(708) = 50.2$	Differences of heat of solution in $\text{PbO}\cdot\text{B}_2\text{O}_3$ melts	[24]
\circ 5	$\Delta H_{m,\mu}(950) = 67$	Heat of crystallization estimated from DTA curves	[17]
\square 6	$\Delta H_{\mu,\alpha}(1020) = 75$	Heat of crystallization estimated from DTA curves	[17]
∇ 7	$\Delta H_{m,c}(1467) = 345.6$	Heat of fusion of orthorhombic cordierite, calculated from $C_p(T)$ values	[20]
All \diamond	$H_m(T-25)$	Heating up to T and dropping into an ice calorimeter	[20]
\blacklozenge 8	$H_m(T-25)$	Heating from 25°C to T by dropping into the calorimeter cell	This work
All \bullet	$H_g(T-25)$	Heating from 25°C to T by dropping into the calorimeter cell	This work
All \blacksquare	$H_\alpha(T-25)$	Heating from 25°C to T by dropping into the calorimeter cell	This work
\bullet 9	$\Delta H_{g,\mu}(25) = 64$	Calculated from consumed heat during heating up to 1200°C	This work
\blacksquare 10	$\Delta H_{\mu,\alpha}(25) = 81$	Calculated from consumed heat during heating up to 1200°C	This work

given by $n_0 = \rho_m N_A / M$ [25] where ρ_m denotes the density of the melt, N_A the Avogadro number and M the molar weight of the molecular building units. In previous papers, iso-stoichiometric crystallization phenomena were the main concern and M was assumed to be the molar weight of the formula unit of the crystalline phase. The first term of Eq. (2), $kT/3\pi\lambda^3\eta(T)$, governs $I(T)$ for large undercooling and can be interpreted as the attachment rate of building units onto the surface of crystalline clusters. At small undercooling the work of forming a critical nucleus, $W(T)$, governs the temperature-dependence of $I(T)$. For spherical nuclei $W(T)$ turns out to be:

$$W(T) = \frac{16\pi V^2 \sigma^3}{3\Delta\mu(T)^2} \quad (3)$$

where σ is the crystal–liquid interfacial free energy, V the molar volume of the crystal phase and $\Delta\mu(T)$ the molar free enthalpy change of crystallization. V is simply given by $V = M/\rho_C$ where ρ_C denotes the density of the crystal phase. For most silicate glasses and for large undercooling ($T_M \geq T \geq 0.5 T_M$) [26], $\Delta\mu(T)$ may be sufficiently approximated according to Hoffman [27] as:

$$\Delta\mu(T) = \Delta H_M T(T_M - T)/T_M^2 \quad (4)$$

where ΔH_M is the molar enthalpy of fusion and T_M the melting temperature. ΔH_M can be obtained from the measured specific heat of fusion, ΔQ , with $\Delta H_M = \Delta Q M$. The interfacial energy σ cannot be measured independently of nucleation experiments. However, one can estimate σ from ΔH_M following an empirical equation of Turnbull [28]:

$$\sigma \approx \alpha \Delta H_M (\rho_c/M)^{2/3} N_A^{-1/3} \quad (5)$$

where α is a constant, if the slight temperature-dependence of σ is neglected. Heterogeneous nucleation starts from nucleating substrates due to their low crystal–substrate interfacial energy $\sigma^* < \sigma$. These substrates can be immersed in the glass matrix or, more likely, placed on the glass surface. The corresponding nucleation rate, $I^*(T)$, is described by means of a reduced work of forming the critical nucleus $W^*(T) = W(T)\Phi$ where $\Phi < 1$ denotes the nucleating activity of the substrate.

4.2. Estimation of parameters

As shown in Eqs. (2)–(5), the magnitude of $I(T)$ is influenced by several parameters which cannot be directly measured: the molar weight of molecular building units, M , the constant α in Eq. (5), the molecular jump distance, λ , and (in the present case of a metastable crystal phase) the melting temperature, T_M . The molar enthalpy of fusion, ΔH_M , can be estimated from Fig. 1 for a given value of M .

4.2.1. M

M is difficult to estimate because cordierite glass is an almost complete network of glass-forming SiO_4^- and AlO_4^- -tetrahedra where one Mg^{2+} ion balances the electric charge of two AlO_4^- -tetrahedra. The same building units are randomly distributed in the framework structures of μ - and α -cordierite, which therefore gives no indications concerning M , also. Thus, only a rough estimate of M was made based on two ideas.

- (1) The building units should be as complex as necessary to allow the stability of AlO_4^- tetrahedra which are present in both the glassy and the crystalline structures. Such building units are assumed to consist of not less than two or three Si- and two Al-tetrahedra which yields, on average, $M \approx 292 \text{ g mol}^{-1}$.
- (2) From the pronounced difference in viscosity between silica and cordierite glass it might be inferred that the viscosity of cordierite glass is mainly controlled by Al–O debonding phenomena. Bearing in mind that the formula unit ($2\text{MgO} \cdot 2\text{Al}_2\text{O}_3 \cdot 5\text{SiO}_2$) includes four AlO_4^- -tetrahedra, the stability of more

complex building units seems to be unlikely. Thus, M should not exceed 585 g mol^{-1} .

4.2.2. α

α is estimated from literature data reviewed in [22] for some silicate glasses where α was calculated from nucleation experiments. The largest value, $\alpha = 0.4$, was found for $\text{BaO} \cdot 2\text{SiO}_2$ glass, the lowest, $\alpha = 0.25$, for $\text{Na}_2\text{O} \cdot 2\text{CaO} \cdot 3\text{SiO}_2$ glass. For $\text{Li}_2\text{O} \cdot \text{SiO}_2$ glass and $\text{Na}_2\text{O} \cdot \text{SiO}_2$ glass $\alpha = 0.31$ and $\alpha = 0.36$, respectively, were reported. Thus, 0.25 and 0.4, respectively, will be used as the upper and lower limits of the possible range of α .

4.2.3. T_M

1467°C and 1300°C are regarded as the largest and lowest possible values of T_M .

4.2.4. λ

λ is assumed to be about $2 \times 10^{-10} \text{ m}$. This is a typical value for silicate glasses [22] being similar to the length of an SiO_4 -tetrahedron of $\approx 2.6 \times 10^{-10} \text{ m}$. Because $I(T)$ does not depend strongly on λ , λ was not varied.

4.3. Homogeneous nucleation rate, $I(T)$

The calculated homogeneous nucleation rate of μ -cordierite, $I(T)$, is shown in Fig. 2 for various parameters (see Table 3) and for experimental density and viscosity data for μ -cordierite and cordierite glass (see 3.1).

The maximum temperature of $I(T)$, T_{max} , can be narrowed to the range 720°C – 920°C . As illustrated by the curves 111 and 211, 112 and 212 or 122 and 222, a scatter of T_{max} of about 90 K is brought about by the experimental uncertainty of the melting temperature, T_M , of $\approx 170 \text{ K}$. Different values of M influence T_{max} up to 30 K (compare curves 112 with 122 or 212 with 222).

Very low values of $I(T)$ below $10^{-60} \text{ m}^{-3} \text{ s}^{-1}$ (Dimensions of nucleation rate and nucleation density data like $[\text{m}^{-3} \text{ s}^{-1}]$, $[\mu\text{m}^{-2}]$ etc. should be read as $[\text{nuclei}/\text{m}^3 \text{ s}]$, $[\text{nuclei}/\mu\text{m}^2]$, etc.) were found in all cases using the upper limit of $\alpha = 0.4$ in Eq. (5), confirming the experimental experience that μ -cordierite nucleates only heterogeneously from the surface. The curves 111 and 211, however, seem to be unlikely because homogeneous volume nucleation rates can be excluded to overcome $10 \text{ m}^{-3} \text{ s}^{-1}$ in the range $T = 100^\circ\text{C}$ – 860°C according to Ref. [3]. The large scatter of $I(T)$ up to 200 orders of magnitude prevents any further predictions concerning the homogeneous nucleation rate of μ -cordierite. As shown in Fig. 2 and Table 3, this scatter results mainly from the uncertainty of α and M while the influence of the experimental uncertainty of T_M^μ and ΔH_M^μ can be neglected.

4.4. Heterogeneous nucleation rate, $I^*(T)$

4.4.1. Surface nucleation density, N^μ

In contrast to volume nucleation, surface-induced nucleation of μ -cordierite can be easily studied by means of optical microscopy. The surface nucleation density, N^μ , was

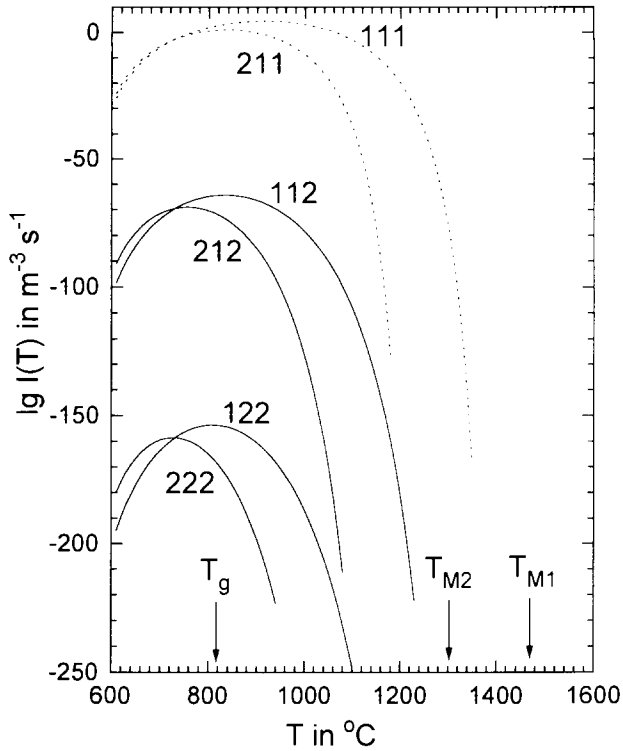


Fig. 2. Calculated steady state homogeneous nucleation rate of μ -cordierite in cordierite glass, $I(T)$, according to Eqs. (2)–(5) for different parameters (see Table 3).

Table 3

Parameters of $I(T)$ curves in Fig. 2. All data refer to the nucleation of μ -cordierite. T_M = melting temperature in $^{\circ}\text{C}$; M = molar weight of molecular building units in g mol^{-1} ; α = constant in Eq. (5); ΔH_M = molar enthalpy of melting in kJ mol^{-1} ; σ = liquid-crystal interfacial energy in mJ m^{-2} ; I_{\max} = maximum nucleation rate in $\text{m}^{-3} \text{s}^{-1}$; T_{\max} = temperature of maximum nucleation rate in $^{\circ}\text{C}$

Curve	T_M	M	α	ΔH_M	σ	$\log I_{\max}$	T_{\max}
111	1467	292	0.25	95	120	4	920
211	1300	292	0.25	85	107	1	830
112	1467	292	0.4	95	193	-64	840
212	1300	292	0.4	85	173	-69	750
122	1467	585	0.4	190	243	-153	810
222	1300	585	0.4	170	217	-159	720

observed in the range 10^{-1} – $10^{-7} \mu\text{m}^{-2}$ for differently prepared surfaces of glasses of the stoichiometric composition of cordierite [6]. Surprisingly, N^{μ} was found not to be essentially influenced by the time and the temperature of thermal nucleation treatment [3–5]. A constant surface nucleation density was also observed in Ref. [7] for

MgO·CaO·2SiO₂ glass surfaces. This effect indicates that surface nucleation is restricted to a limited number of nucleation sites which are completely exhausted before any crystal can reach detectable size [8]. Thus, N^μ simply represents the number density of these nucleation sites, N_0^μ , which was found to be $\approx 10^{-4} \mu\text{m}^{-2}$ for fractured [4] and mechanically polished [9,10] cordierite glass surfaces. Experiments made under dust-protecting efforts (fracture and thermal treatment under vacuum or in a glove box) indicate that active nucleation sites are mainly related to solid foreign particles (dust) [6].

4.4.2. Surface nucleation rate, dN^μ/dt

Despite the constancy of N^μ , it was possible to calculate the surface nucleation rate, dN^μ/dt , from the observed distribution of sizes of μ -cordierite crystals [8–10]. The ‘birth-time’ of crystals was calculated from their size, enabling calculation of the time-dependent surface nucleation rate $dN^\mu(t)/dt$ that occurs until the saturation state is reached at N_0^μ . The maximum values of dN^μ/dt for a given temperature are shown in Fig. 3 (curve 5). For the sake of comparison with other surface nucleation phenomena, directly measured surface nucleation rate data presented in previous literature are also shown (curves 1–4). Despite the strong saturation effect of the μ -cordierite surface nucleation, the maximum values lie in the scatter of other data. The most noticeable

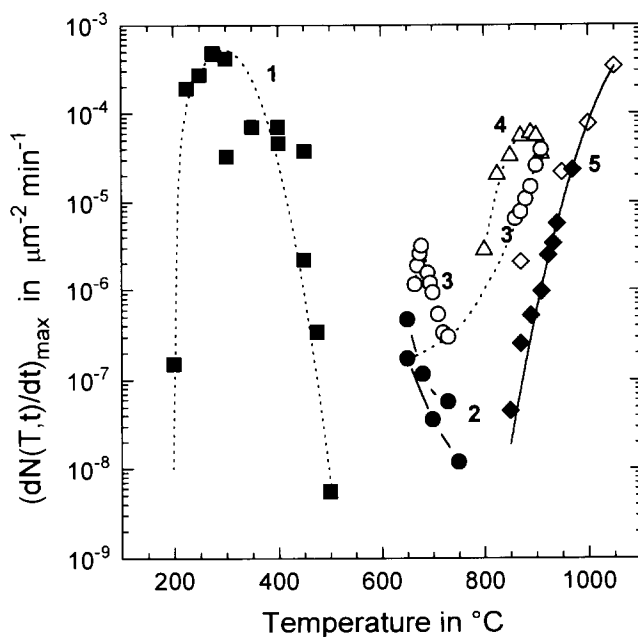


Fig. 3. Maximum nucleation rate of μ -cordierite, dN^μ/dt_{max} , at fractured (curve 5, \diamond [8]) and mechanically polished (curve 5, \blacklozenge [10]) cordierite glass surfaces obtained from crystal size distribution data. For the sake of comparison, directly measured surface nucleation rates presented in previous literature are shown (curves 1–4, see Table 4 for symbols).

difference is that dN^u/dt steadily increases up to 1050°C, which is 235 K above the glass transition temperature at 815°C, without reaching a maximum. Similar behaviour was reported for the nucleation of cristobalite at float glass surfaces [29] (see curve 3 in Fig. 3 at $T > 850^\circ\text{C}$). Directly measured surface nucleation data are listed in Table 4.

4.4.3. Heterogeneous nucleation rate, $I^*(T)$

In order to discuss the temperature-dependence of dN^u/dt_{max} data shown in Fig. 3, each surface nucleation site was considered as being surrounded by an active layer of melt where heterogeneous nucleation can occur. The layer thickness was assumed to be of the dimension of the molecular jump distance $\lambda \approx 2 \times 10^{-10}$ m. The layer volume was obtained by multiplying λ by the substrate–melt interface area, A . A was roughly estimated from the density number of active nucleation sites $N_0^u \approx 10^{-4} \mu\text{m}^{-2}$ assuming that these sites are spheres of about $2R \approx 10 \mu\text{m}$ in size being half embedded in the melt. In this sense, a “heterogeneous volume nucleation” rate, $I^*(T)$, was calculated from Fig. 3 making it possible to compare homogeneous and heterogeneous nucleation rate data and to discuss the influence of the activity of surface nucleation sites on the temperature behaviour of nucleation.

$I^*(T)$ values obtained by this way are shown as points in Fig. 4. The lowest curve, $I(T)_{112}$, is the homogeneous nucleation rate already shown in Fig. 2 (curve 112). The upper curves, $I^*(T)$ were calculated from $I(T)_{112}$ using reduced values for the work of forming a critical nucleus, $W^*(T) = \sigma W(T)_{112}$. With decreasing Φ the maximum temperature of nucleation increases up to the vicinity of T_M^u and $\exp(-W^*(T)/kt)$ is ≈ 1 even for small undercooling. Thus, the viscosity can govern the temperature-dependence of $I^*(T)$ resulting in smoother temperature-dependence of $I(T)$. This effect was previously pointed out by Zanotto [32] to cause a constant nucleation density which was found in [3–5, 7]. Nevertheless, as shown in Fig. 3, $I^*(T)$ still depends substantially on temperature. However, due to the increased nucleation activity at high temperatures, both essential nucleation and growth rates can occur simultaneously. In the present case, this second effect must be regarded as being mainly responsible for the observed constant value of N^u .

A good fit of experimental points in Fig. 4 can be attained assuming $T_M^u = 1467^\circ\text{C}$ for all sets of parameters where $\sigma\Phi^{1/3} \approx 100 \text{ mJ m}^{-2}$ is valid. For the possible range of σ (see Table 3 in Section 4.3) this condition is fulfilled for Φ in the range 0.15–0.05. On the basis of $I(T)_{112}$, (curve 112 in Fig. 2; see Table 3 for parameters), the best fit was

Table 4
Directly measured surface nucleation data (curves 1–4 in Fig. 3)

Curve	Points	Glass	Surface	Crystal	Ref.
1	■	$\text{Na}_2\text{O} \cdot 2\text{SiO}_2$	Fire-polished	$\text{Na}_2\text{Si}_2\text{O}_5$	[30]
2	●	Soda-lime	Fire-polished	“123”	[31]
3	○	Float	Fire-polished	Cristobalite	[29]
4	△	Cordierite	Mechanically polished	“X-phase”	[3]

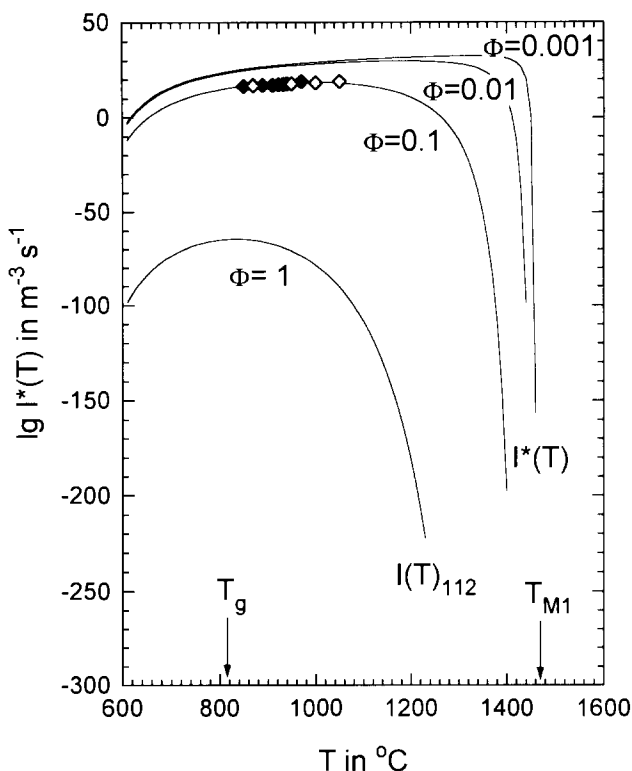


Fig. 4. Influence of the activity of surface nucleation sites, Φ (curve parameters), upon the temperature-dependence of nucleation. $I(T)_{112}$: homogeneous nucleation rate already shown in Fig. 2; $I^*(T)$: calculated from $I(T)_{112}$ for differently reduced values for the work of forming a critical nucleus $W^* = W(T)_{112}\Phi$. The points were calculated from dN^*/dt_{\max} data (Fig. 3, curve 5).

found for $\Phi = 0.1$. It was not possible, however, to fit the experimental points with $T_M^* = 1300^\circ\text{C}$. This result indicates that the virtual melting temperature of μ -cordierite is rather close to the melting temperature of orthorhombic cordierite.

Acknowledgements

Financial support of the Deutsche Forschungsgemeinschaft is grateful acknowledged. The investigation presented here is closely related to a cooperative effort of the TC7 of the ICG to advance the understanding of surface nucleation phenomena. Helpful discussions and advice from the TC7 chairman W. Pannhorst and from I. Donald, W.M. Fokin, W. Höland, K. Heide, I. Szabo, G. Völksch and E.D. Zanotto were much appreciated.

References

- [1] W. Schreyer and J.F. Schairer, *Z. Kristallogr.*, 116 (1961) 60–82.
- [2] A. Putnis, *Mater. Sci. Forum*, 7 (1986) 63–72.
- [3] N.S. Yuritsin, V.M. Fokin, A.M. Kalinina and V.M. Filipowich, *Proc. Nat. Conf. Glassy State*, St. Petersburg, 1986, pp. 235–236.
- [4] R. Müller and D. Thamm, *Wiss. Beitr. Friedrich-Schiller-Univers. Jena*, 4th Intern. Otto-Schott-Coll. (1990), pp. 86–87.
- [5] K. Heide, G. Völksch and Chr. Hanay, *Proc. XVI Intern. Congr. Glass*, Madrid 1992, Vol. 5, pp. 111–116.
- [6] R. Müller, S. Reinsch and W. Pannhorst, *Chem. Commun. Bulg. Acad. Sci., Proc. 11th Conf. Glass Ceram.*, Varna 1993, 63–68.
- [7] E.D. Zanotta and R. Basso, *Ceramica (Sao Paulo)*, 32 (1986) 117–120.
- [8] S. Reinsch, R. Müller and W. Pannhorst, *Proc. 2nd Annu. Meeting Arbeitskreis Nichtkrist. and Partiiellkrist. Strukt.*; Heubach 1993, 139–143.
- [9] V.M. Fokin, Lecture at the annual meeting of TC7 of ICG in Madrid, October 1992; results are given in Ref. [10].
- [10] V.M. Fokin, N.S. Yuritsin, A.M. Kalinina, V.M. Filipowich and D.N. Filippova, *Proc. 5th Int. Otto-Schott-Coll.*, 1994, *Glastech. Ber. Glass Sci. Technol.* 67C, 392–395.
- [11] R. Müller, T. Hübert and M. Kirsch, *Silikattechnik*, 37 (1986) 111–114.
- [12] R. Naumann and D. Petzold, *J. Therm. Anal.*, 20 (1981) 319.
- [13] N.A. Sirashiddinov, *Usbek. Chim. J.*, (1966) 9–11.
- [14] T.I. Barry, J.M. Cox and R. Morell, *J. Mater. Sci.*, 13 (1978) 594–610.
- [15] W. Zdaniewski, *J. Mater. Sci.*, 8 (1973) 192–202.
- [16] M.D. Karkhanavala and F.A. Hummel, *J. Am. Ceram. Soc.*, 36 (1953) 389–392.
- [17] I. Uei, K. Inoue and M. Fukui, *J. Ceram. Assoc. Jpn.*, 74 (1966) 325–335 (in Japanese).
- [18] Y. Hirose, H. Doi, O. Kamigaito, *J. Mater. Sci. Lett.*, 3 (1984) 153–155.
- [19] H. Fischer, D. Sporn, R. Müller and H. Bertagnolli, *Proc. 2nd Ann. Meeting Arbeitskreis Nichtkrist. and Partiiellkrist. Strukt.*; Heubach 1993, 133–138.
- [20] Y. Bottinga and P. Richet, *Earth and Planetary Sci. Lett.*, 3 (1984) 415–432.
- [21] R.A. Robie, B.S. Hemingway and J.R. Fischer, *US Geol. Surv. Bull.*, 1452 (1978) 456.
- [22] P.F. James, *J. Non-Cryst. Solids*, 73 (1985), 517–540.
- [23] A. Navrotsky and O.J. Cleppa, *J. Am. Ceram. Soc.*, 56 (1973) 198–199.
- [24] M.A. Carpenter, A. Putnis, A. Navrotsky, J. Desmond and C. McConnell, *Geochim. Cosmochim. Acta*, 47 (1983) 899–898.
- [25] G.F. Neilson and M.C. Weinberg, *J. Non-Cryst. Solids*, 34 (1979) 137–147.
- [26] I. Gutzow, *Cont. Phys.*, 21 (1980) 121–137.
- [27] J.D. Hoffman, *J. Chem. Phys.*, 29 (1958) 1192.
- [28] D. Turnbull, *J. Appl. Phys.*, 21 (1950) 1022.
- [29] J. Deubner, R. Brückner and H. Hessenkemper, *Glastechn. Ber.*, 65 (1992) 256–266.
- [30] K. Thakahashi and T. Sakaino, *Bull. Tokyo Inst. Technol.*, 104 (1971) 1–26 (in Japanese).
- [31] Z. Strnad and R.W. Douglas, *Phys. Chem. Glasses*, 14 (1973) 33–36.
- [32] E.D. Zanotto, *Ceramic Transactions: Nucleation and Crystallization in Liquids and Glasses*, Am. Ceram. Soc., 30 (1993) 65–74.